

Influence of thermal annealing on the dielectric properties and electrical relaxation behaviour in nanostructured CoFe_2O_4 ferrite

This article has been downloaded from IOPscience. Please scroll down to see the full text article.

2007 J. Phys.: Condens. Matter 19 386201

(<http://iopscience.iop.org/0953-8984/19/38/386201>)

View [the table of contents for this issue](#), or go to the [journal homepage](#) for more

Download details:

IP Address: 129.252.86.83

The article was downloaded on 29/05/2010 at 04:42

Please note that [terms and conditions apply](#).

Influence of thermal annealing on the dielectric properties and electrical relaxation behaviour in nanostructured CoFe_2O_4 ferrite

N Sivakumar¹, A Narayanasamy^{1,3}, C N Chinnasamy^{2,4} and B Jeyadevan²

¹ Materials Science Centre, Department of Nuclear Physics, University of Madras, Guindy Campus, Chennai 600 025, India

² Graduate School of Environmental Studies, Tohoku University, Sendai 980-8579, Japan

E-mail: ansjourn@rediffmail.com

Received 21 March 2007, in final form 19 July 2007

Published 29 August 2007

Online at stacks.iop.org/JPhysCM/19/386201

Abstract

Nanocrystalline cobalt ferrite particles with the grain size of 8 nm were synthesized by using the co-precipitation technique and subsequently heat treated to obtain larger grain sizes. The effect of grain size, cation distribution, frequency and temperature on their dielectric properties has been studied. The dielectric constant (ϵ') of 8 nm grains is found to be an order of magnitude higher and the dielectric loss ($\tan \delta$) is an order of magnitude smaller compared to those of the micron-size particles. The dielectric relaxation is found to be non-Debye in nature with the activation energy decreasing with thermal annealing due to structural perfection.

1. Introduction

In recent decades, nanometre-scale particles have attracted great interest in fundamental science and also in technological applications. Nanoparticles generally have some novel and/or enhanced physical and chemical properties [1, 2]. Spinel ferrites are one of the most significant magnetic materials which have been extensively used in modern electronic technologies [3, 4]. Nanoparticles of spinel ferrites are of practical interest in a wide range of applications like high-density magnetic information storage, magnetic resonance imaging, targeted drug delivery, etc [5, 6]. Spinel ferrites have high electrical resistivities and low eddy current and dielectric losses. Cobalt ferrite is one of the potential candidates for magnetic and magneto-optical recording media [7–10]. Dielectric behaviour is one of the most significant properties of ferrites which clearly depend on the preparation conditions, sintering temperature, composition and

³ Author to whom any correspondence should be addressed.

⁴ Present address: Department of Electronics and Computer Engineering, Northeastern University, 360 Huntington Avenue, Boston, MA 02115, USA.

the grain size [11–13]. Dielectric studies provide important information on the behaviour of localized electric charge carriers, which give rise to a better understanding of the mechanism of dielectric polarization.

The ideal inverse spinel structure of bulk cobalt ferrite is $(\text{Fe})_A[\text{CoFe}]_B\text{O}_4$, where A and B refer to ions with tetrahedral and octahedral site symmetry, respectively. Recently, cobalt ferrites have been shown to exhibit interesting magnetic properties in the nanocrystalline form compared with those of micrometre-size grains [14–18]. Giri *et al* [18] have observed structural disorder, enhanced optical absorption and high coercivity with the reduction of grain size in nanocrystalline cobalt ferrite. Several reports are available in the literature on the electrical conductivity and dielectric properties of bulk cobalt ferrite [19–22]. Jonker [20] has studied the electrical properties of a series of bulk $\text{Co}_{3-x}\text{Fe}_x\text{O}_4$ ferrites and observed two regions of conductivity. The hole hopping between Co^{II} and Co^{III} ions contributes to the low-conductivity region and the electron hopping between Fe^{2+} and Fe^{3+} ions is found to be responsible for the high-conductivity region. Na *et al* [21, 22] have reported the mechanism for electrical conduction for bulk CoFe_2O_4 under various heat treatment conditions. They have also observed a decrease in electrical resistivity with quenching temperature, which is mainly because of the decrease in grain boundary resistance in Fe-excess cobalt ferrites. However, to our knowledge, there is no report available in the literature on the dielectric behaviour of nanostructured CoFe_2O_4 . This has motivated us to carry out dielectric studies on nanostructured CoFe_2O_4 , and the aim of the present work is to study the effect of grain size on the dielectric properties of cobalt ferrite in the nanoregime. Moreover, the electrical relaxation data have been analysed using modulus spectroscopy to investigate whether nanocrystalline cobalt ferrite exhibits Debye-type or non-Debye-type relaxation.

2. Experimental details

2.1. Preparation and phase identification

Cobalt ferrite was prepared using the co-precipitation technique [23], and the x-ray diffraction (XRD) pattern confirmed the formation of spinel phase without any impurity phase, as reported in our earlier paper [24]. To attain various grain sizes, the as-prepared sample was heat treated at 1473 K for different durations such as 2 and 10 h. The average grain sizes were determined from the full width at half maximum of the (311) reflection of the XRD patterns using Scherrer's formula [25]. For convenience the samples are labelled as A for the as-prepared sample, B for the sample annealed at 1473 K/2 h and C for the sample annealed at 1473 K/10 h. The average grain sizes of samples A–C were 8, 92 and 123 nm respectively.

2.2. Characterization

The dielectric properties of nanocrystalline cobalt ferrite were studied as a function of both frequency and temperature in the range 1 Hz–10 MHz and 300–823 K respectively, using an impedance/gain phase analyser (Solartron 1260) with a personal computer and software to acquire the impedance data. For these measurements, the sample was made in the form of a pellet and the pellet was sandwiched between two platinum electrodes. The sample heating rate was 2 K min^{-1} for the impedance measurements. The temperature was measured with an accuracy of $\pm 1 \text{ K}$ using a Eurotherm (818 P) proportional-integral-derivative (PID) temperature controller. Both the dielectric constant, ϵ' , and dielectric loss, $\tan \delta$, as well as the real (M') and imaginary (M'') parts of the complex electric modulus, M^* , were calculated using the raw data of Z' and Z'' and the sample dimensions. Scanning electron micrographs were recorded using a LEO Stero Scan 440 scanning electron microscope (SEM).

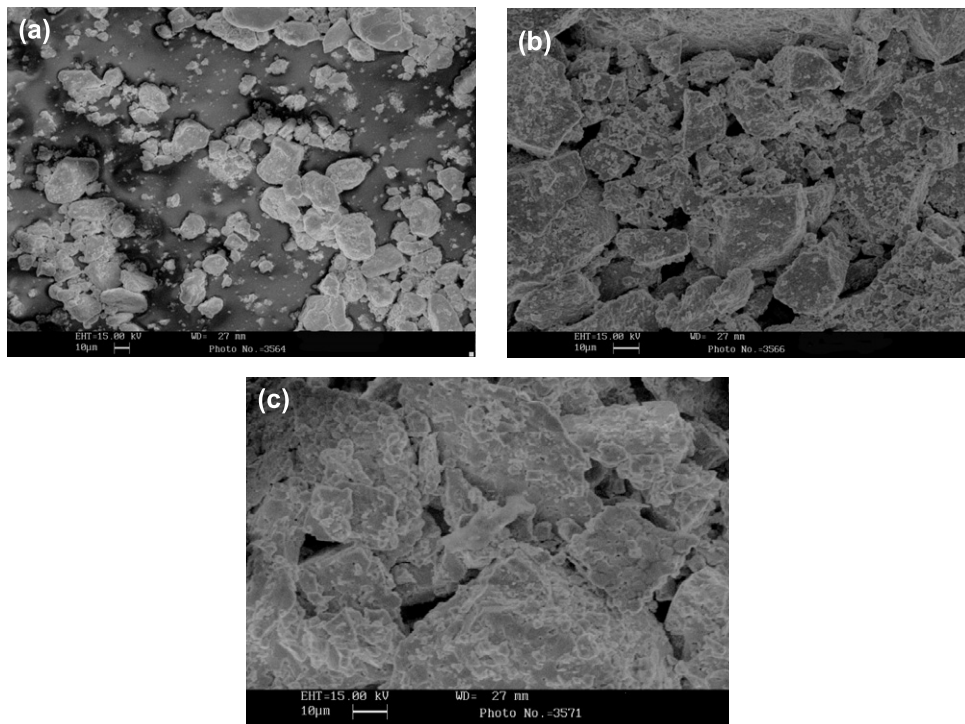


Figure 1. SEM pictures of CoFe_2O_4 : (a) sample A, (b) sample B and (c) sample C.

3. Results and discussion

3.1. Surface morphology

Figures 1((a)–(c)) show the microstructure of cobalt ferrite for samples A–C respectively. All the samples have micron-sized particles, as seen from the SEM picture, with clear evidence of an increase in particle size with annealing temperature. The particle size of sample A is found to lie in the range 11–18 μm . In the case of samples B and C, the particles are found to be slightly agglomerated, and the particle sizes are around 20–35 and 40–60 μm respectively. The SEM micrographs also show an improvement in the structural homogeneity with heat treatment.

3.2. Variation of dielectric constant and dielectric loss with frequency

The effect of frequency on the real part of the dielectric constant ϵ' at 473 K for different grain sizes is illustrated in figure 2(a). The value of ϵ' decreases with frequency, which is a normal dielectric behaviour in ferrites. The decrease in ϵ' takes place when the jumping frequency of the electric charge carriers cannot follow the alternation of ac electric field beyond a certain critical frequency [26]. Variations in dielectric constant of ferrites have been mainly attributed to the variations in the concentration of Fe^{2+} ions [27–29]. The greater the concentration of these ions, the higher the dielectric constant expected. The presence of Fe^{2+} ions results in charge transfer of the type $\text{Fe}^{2+} \leftrightarrow \text{Fe}^{3+}$ ions, causing a local displacement of electrons in the direction of the electric field leading to polarization. Mahajan *et al* [19] have observed that the real part ϵ' of the dielectric constant is of the order of 10^2 at 473 K at a frequency of 1 kHz for bulk cobalt ferrite. In the present study, the real part of dielectric constant for sample A

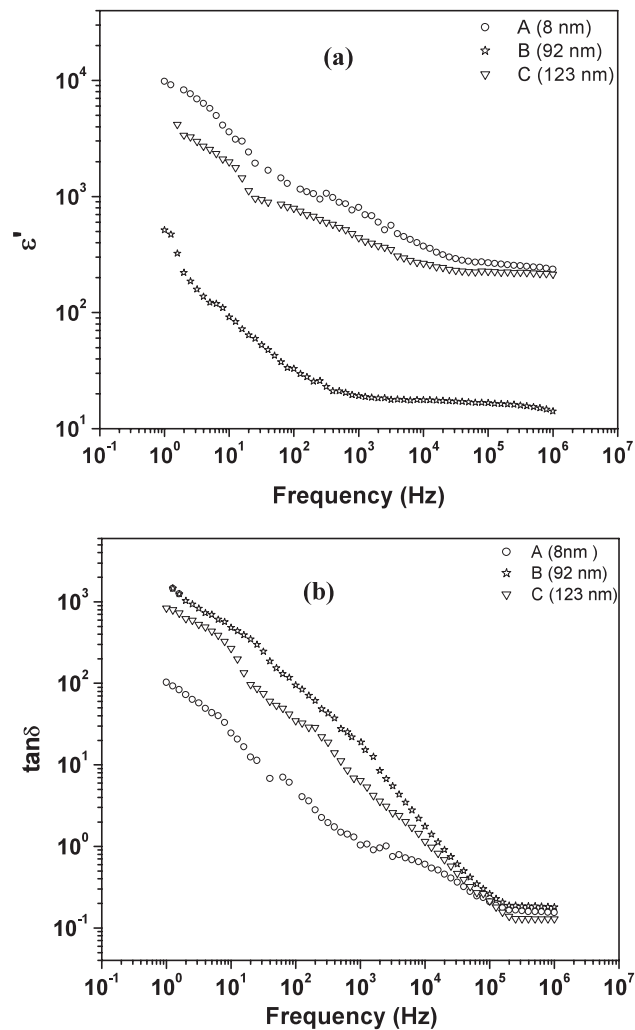


Figure 2. (a) The real part of the dielectric constant (ϵ') at 473 K as a function of frequency for different grain sizes of a CoFe_2O_4 sample. (b) The dielectric loss factor ($\tan\delta$) at 473 K as a function of frequency for different grain sizes of a CoFe_2O_4 sample.

is of the order of 10^3 at the same temperature and frequency, which is an order of magnitude higher compared to that of bulk cobalt ferrite [19]. Because of the higher dielectric constant, the 8 nm particles are highly suitable for microwave applications. Moreover, the dielectric constant decreases by more than an order of magnitude when the grain size increases from 8 to 92 nm. This is due to the reduction of $\text{Fe}^{2+} \leftrightarrow \text{Fe}^{3+}$ pairs in B sites as a consequence of the decrease in the number of iron ions in B sites, as revealed by the in-field Mössbauer studies reported in our earlier work [24]. We have observed a 6% reduction of iron ions in B sites upon thermal annealing of the as-prepared sample at 1473 K for 2 h [24]. But, the dielectric constant increases significantly when the grain size is increased to 123 nm by further annealing (sample C). Moreover, our in-field Mössbauer study [24] clearly shows that the cation distribution does not change when the grain size increases from 92 to 123 nm. Hence, the increase in the value of dielectric constant for sample C is not because of the cation distribution. A longer

Table 1. The values of dielectric constant (ϵ'), dielectric loss ($\tan \delta$) and resistivity for CoFe_2O_4 spinel ferrite samples measured at 473 K.

Sample (grain size in nm)	ϵ' at 1 kHz	$\tan \delta$ at 1 kHz	Resistivity (ρ) (Ω cm)
A (8)	737.1	1.0	4.4×10^5
B (92)	19.0	21.9	3.9×10^6
C (123)	421.6	6.4	6.0×10^5

duration of annealing of sample C for 10 h at 1473 K might have reduced some of the Fe^{3+} ions into Fe^{2+} ions [30], which leads to an enhancement in the number of electron hoppings and thus an increase in dielectric polarization and ϵ' . This also accounts for the smaller value of resistivity of sample C compared to that of sample B. Of course, the higher grain size of sample C will also reduce the resistivity. An improvement in structural homogeneity with annealing, as observed from SEM micrographs, might have also contributed to the increase in ϵ' . A similar observation has also been made in nickel–zinc ferrites which were prepared by the citrate precursor method [31].

Plots of the dielectric loss ($\tan \delta$) as a function of frequency for the three grain sizes are shown in figure 2(b). Normally, the dielectric loss in ferrites is a measure of lag in the polarization with respect to the alternating field. Shitre *et al* [32] have observed that $\tan \delta$ is around 0.4 at 300 K at a frequency of 1 kHz for bulk cobalt ferrite prepared by the ceramic method. In the present study, $\tan \delta$ for sample A (8 nm) is about 0.03 at 300 K in the same frequency range. The dielectric loss is thus found to be an order of magnitude lower for the 8 nm particles compared to that of bulk cobalt ferrite [32]. Sample A (8 nm) is, therefore, suitable for microwave applications because of the low dielectric losses. The behaviour of $\tan \delta$ in ferrites is normally reflected in the resistivity measurements, with the high-resistivity materials exhibiting low dielectric losses and vice versa [33]. However, a reverse trend is observed in the present work for samples B (92 nm) and C (123 nm), as seen from table 1. Our extended x-ray absorption fine-structure (EXAFS) studies [24] show an increase in the concentration of cobalt ions and a decrease in the concentration of iron ions in octahedral sites in samples B and C compared to that in sample A. The presence of cobalt ions gives rise to hole hopping ($\text{Co}^{\text{II}} \leftrightarrow \text{Co}^{\text{III}}$), whose hopping rate should be smaller than that of electron hopping. Since the contribution of hole hopping is relatively larger in samples B and C, the dielectric loss is higher for these two samples even though their resistivities are higher. For sample C (123 nm), both the dielectric loss and resistivity are smaller in value compared to those of sample B, and this may be attributed to structural improvement with further annealing for a long duration, as revealed by the SEM studies.

3.3. Variation of dielectric constant and dielectric loss with temperature

The temperature dependence of the dielectric constant and dielectric loss for all the grain sizes are shown in figures 3((a) and (b)) respectively. Both the dielectric constant and dielectric loss increase with temperature for all the grain sizes, which is generally an expected result for ferrites [13, 34]. The mobility of charge carriers, and hence their hopping rate, increases with temperature. The dielectric polarization, therefore, increases, causing an increase in dielectric constant and dielectric loss with temperature. The temperature-dependent dispersion of the dielectric constant is quantitatively expressed by the following equation [35],

$$\epsilon' - \epsilon_{\infty} = \frac{\epsilon_0 - \epsilon_{\infty}}{1 + \omega^2 \tau^2}, \quad (1)$$

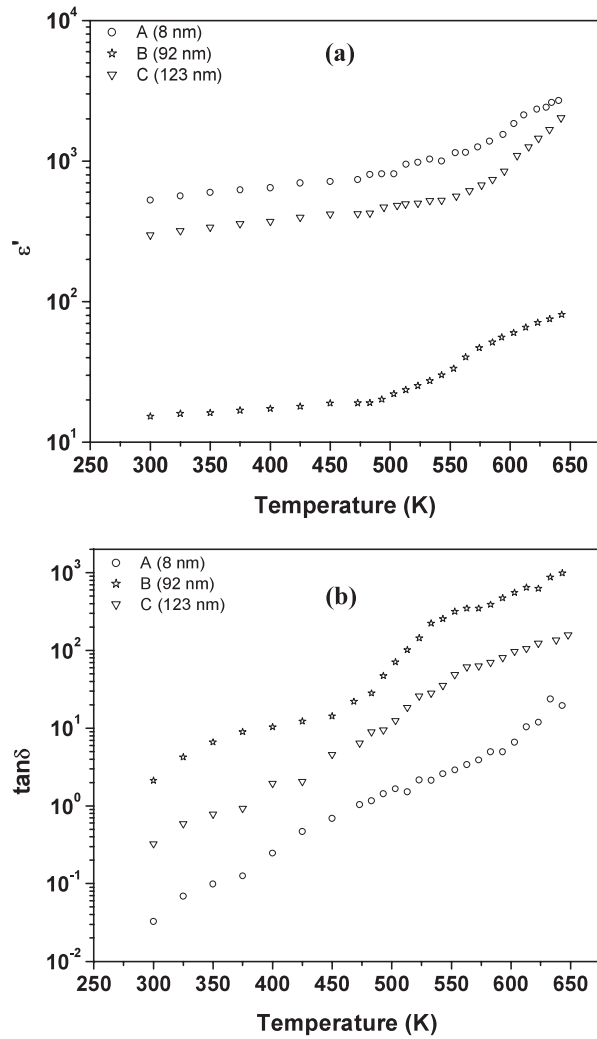


Figure 3. (a) The temperature dependence of the dielectric constant (ϵ') for various grain sizes of a CoFe₂O₄ sample at 1 kHz. (b) The temperature dependence of the dielectric loss factor ($\tan \delta$) for various grain sizes of a CoFe₂O₄ sample at 1 kHz.

where ϵ' is the dielectric constant at frequency ω , ϵ_0 and ϵ_∞ are respectively low-frequency and high-frequency dielectric constants, and τ is the relaxation time. The relaxation time decreases with temperature due to high thermal energy supplied to the sample, and hence the dielectric constant increases with temperature. The temperature dependence of the dielectric loss is given by

$$\tan \delta = \frac{\epsilon''}{\epsilon'} = \frac{(\epsilon_0 - \epsilon_\infty)\omega\tau}{\epsilon_0 - \epsilon_\infty\omega^2\tau^2}. \quad (2)$$

As τ decreases with temperature, the dielectric loss increases, as we observed.

Figure 4(a) shows the temperature dependence of ϵ' at selected frequencies for sample A. The temperature dependence of the dielectric constant is different for different frequencies, which can be explained as detailed below. In general, the dielectric constant in ferrites is

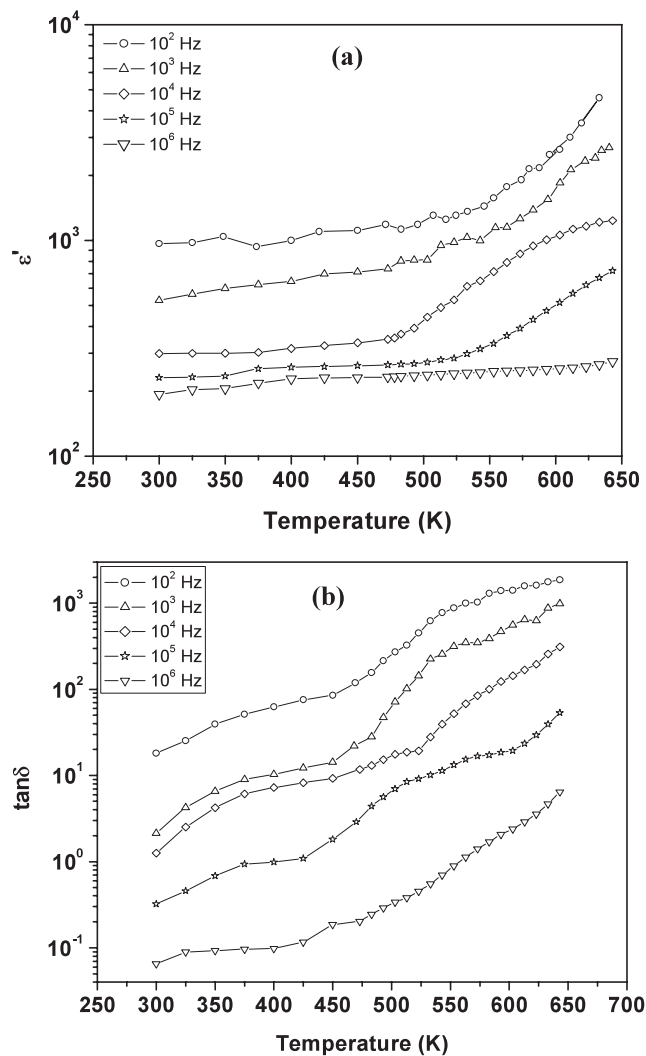


Figure 4. (a) The temperature dependence of the dielectric constant (ϵ') for sample A of CoFe_2O_4 at selected frequencies. (b) The temperature dependence of the dielectric loss factor ($\tan\delta$) for sample C of CoFe_2O_4 at selected frequencies.

attributed to four types of polarization (interfacial, dipolar, atomic and electronic). All these polarizations would contribute to the dielectric constant at low frequencies. The dielectric constant increases with temperature at all frequencies, the increase being quite significant at low frequencies [35]. The rapid increase in the dielectric constant in the high-temperature region at low frequencies is mainly due to interfacial and dipolar polarizations. Both these polarizations are highly frequency dependent, falling rapidly with frequency. At high frequencies only the electronic and ionic polarizations prevail, and they are frequency independent. This explains the observed temperature dependence of the dielectric constant at various frequencies. The variation of dielectric loss ($\tan\delta$) as a function of temperature at selected frequencies (figure 4(b)) has been investigated. Its behaviour is similar to that of the dielectric constant, which can be also explained as in the case of the dielectric constant.

3.4. Electrical modulus studies

The use of the modulus formalism has the advantage of suppressing the electrode polarizing effects [13, 36–38]. The complex electrical modulus, M^* , is related to the complex dielectric constant, ε^* , by the relation [38]

$$M^* = 1/\varepsilon^* = M' + iM'' \quad (3)$$

The modulus data were fitted with the KWW (Kohlrausch, Williams and Watts) function [39] and the stretched exponent, β , and the dielectric relaxation time, τ , were obtained. The electrical modulus is defined [38] as the electric analogue of the dynamical mechanical modulus and is related to the complex permittivity $\varepsilon^*(\omega)$ by

$$M^*(\omega) = \frac{1}{\varepsilon^*(\omega)} = \{\varepsilon'(\omega) - i\varepsilon''(\omega)\}[\varepsilon^*(\omega)]^2 = M'(\omega) + iM''(\omega), \quad (4)$$

where $M'(\omega)$ and $M''(\omega)$ are the real and imaginary parts of the electrical modulus, and $M_\infty = 1/\varepsilon_\infty$ is the inverse of the high-frequency dielectric permittivity.

The modulus, in fact, can be written in terms of the Fourier transform of the time derivative of an electrical relaxation function,

$$\phi(t) = M_\infty \left[1 - \int_0^\infty e^{-i\omega t} \left\{ \frac{d\phi}{dt} \right\} dt \right]. \quad (5)$$

The function $\phi(t)$ gives the time evolution of the electric field within the dielectrics and is related to the relaxation time by the decay function proposed by Kohlrausch, Williams and Watts (KWW) [39] and is given by

$$\phi(t) = \exp \left[- \left(\frac{t}{\tau_m} \right)^\beta \right], \quad 0 < \beta < 1, \quad (6)$$

where τ_m is the most probable relaxation time and β is the stretched exponent parameter. The value of β indicates whether the relaxation in a given material is Debye or non-Debye in nature and it is related to the full width at half maximum of a suitably normalized $M''(\omega)$ versus ω curve.

Figure 5(a) shows the imaginary part of the electrical modulus for nanocrystalline cobalt ferrite for various grain sizes measured at 623 K. In the figure, the continuous lines represent the fitted curves, whereas the symbols represent the experimental data. The value of the stretched exponent parameter β is given in figure 5(a) and it is less than one for all grain sizes. For an ideal dielectric, the value of β is equal to 1, for which the dipole–dipole interaction is negligible. But, for a system in which dipole–dipole interaction is significant, the β value is always less than 1 [40]. Figure 5(b) shows the imaginary part of modulus (M'') spectra of sample C at selected temperatures. The figure clearly shows that the M'' peak shifts towards higher frequency with temperature. The peak frequency is called the relaxation frequency and it increases with temperature because of the thermal activation of the localized electric charge carriers which form the electric dipoles. Figure 6 gives the variation of the relaxation time (τ) versus temperature for samples A–C. It is observed that the relaxation time decreases with the measuring temperature. The electric dipoles in ferrites originate from hopping of charge carriers. When the charge carriers are thermally activated, the hopping rate increases and hence the relaxation time decreases with temperature. The temperature dependence of the relaxation time is fitted with the following equation:

$$\tau = \tau_0 \exp \left(\frac{-E}{k_B T} \right), \quad (7)$$

where E is the activation energy of the relaxation process, k_B is the Boltzmann constant and τ_0 is the maximum relaxation time [41]. The data could be fitted with a single straight line,

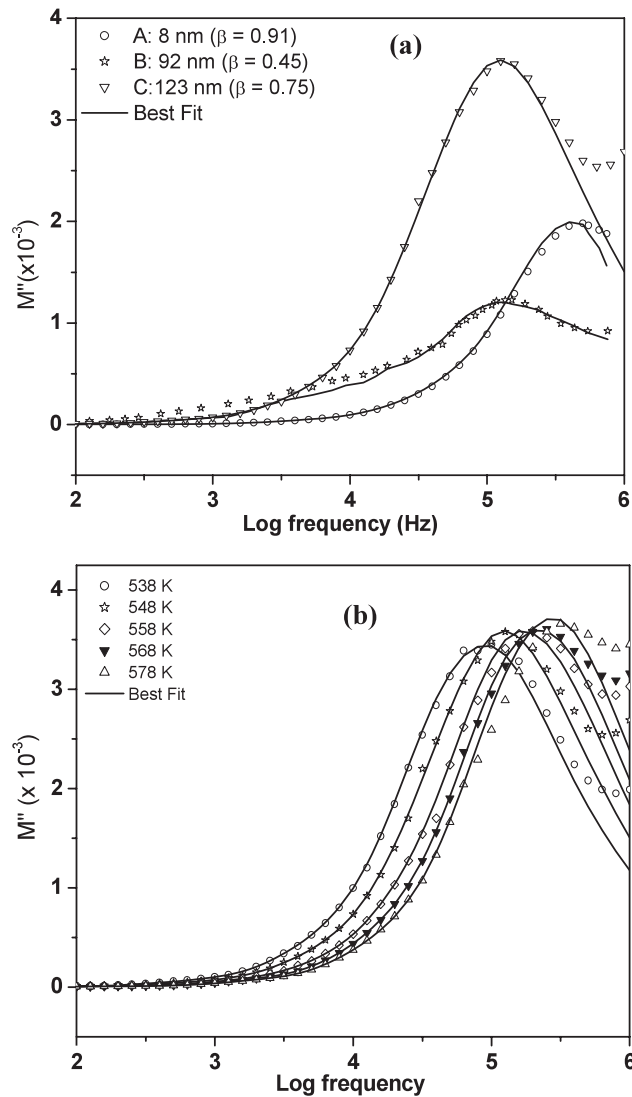


Figure 5. (a) The imaginary part of the modulus (M'') spectra for different grain sizes of a CoFe_2O_4 sample measured at 538 K. The solid curves are the best fits to equation (3). (b) The imaginary part of the modulus (M'') spectra of sample C of CoFe_2O_4 at selected temperatures. The solid curves are the best fits to equation (3).

suggesting that there is only one type of relaxation process. The activation energy decreases with thermal annealing, and this may be due to improvement in the microstructural perfection on annealing. Also, we observe that the relaxation time increases with thermal annealing at 1473 K. Our EXAFS measurements [24] have clearly indicated that the number of Co^{2+} ions in B sites increases and the number of Fe^{3+} ions decreases with annealing. Since the hole hopping arising from the $\text{Co}^{\text{II}} \leftrightarrow \text{Co}^{\text{III}}$ transition is expected to be slower than the electron hopping, the relaxation time increases with annealing.

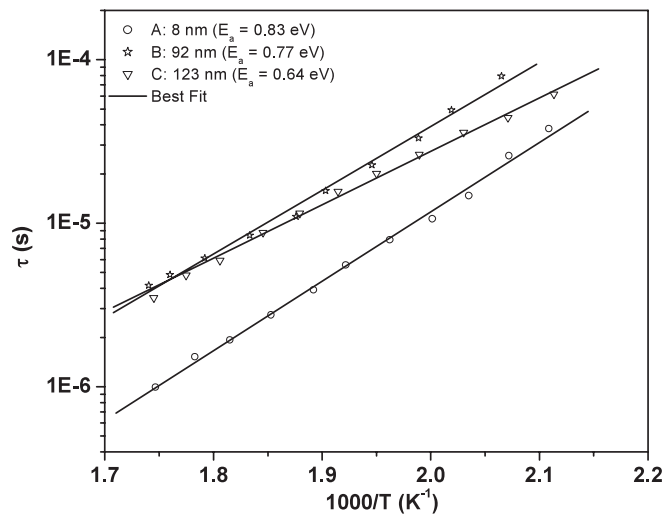


Figure 6. The variation of dielectric relaxation time with temperature for CoFe_2O_4 for various grain sizes.

4. Conclusion

The dielectric behaviour of nanocrystalline CoFe_2O_4 has been studied. The real part of the dielectric constant (ϵ') for the 8 nm grain size sample is found to be an order of magnitude higher than that of bulk cobalt ferrite. The observed decrease in dielectric constant when the grain size is increased from 8 to 92 nm is clearly due to the predominant effect of migration of some of the Fe^{3+} ions from octahedral to tetrahedral sites. The dielectric relaxation in nanocrystalline CoFe_2O_4 exhibits non-Debye behaviour, with the value of β being less than one for all the grain sizes. The activation energy for dielectric relaxation is found to decrease for the annealed samples due to structural ordering. The present study shows that the dielectric properties can be tailor-made to suit the requirement of a particular application by controlling the grain size and the cation distribution.

Acknowledgment

The financial support from DST, Government of India (Sanction No. SR/S5/NM-23/2002) is acknowledged.

References

- [1] Siegel R W 1993 *Phys. Today* **46** 64
- [2] Service R F 1996 *Science* **271** 920
- [3] Gillot B 1998 *Eur. Phys. J. AP* **4** 243
- [4] Sugimoto M 1999 *J. Am. Ceram. Soc.* **82** 269
- [5] Lübke A S, Bergemann C, Brock J and McClure D G 1999 *J. Magn. Magn. Mater.* **194** 149
- [6] Bulte J W M, de Cuyper M, Despres D and Frank J A 1999 *J. Magn. Magn. Mater.* **194** 204
- [7] Suzuki Y, van Dover R B, Gyorgy E M, Philips J M, Korenivski J, Werder J, Chen C H, Cava R J, Krajewski J J, Peck W F and Do K B 1996 *Appl. Phys. Lett.* **68** 714
- [8] Cheng F X, Jia J T, Xu Z G, Zhou B, Liao C S, Yan C H, Chen L Y and Zhao H B 1999 *J. Appl. Phys.* **86** 2727
- [9] Kitamoto Y, Kantake S, Shirasaki A, Abe F and Naoe M 1999 *J. Appl. Phys.* **85** 4708
- [10] Fontijn W F J, van der Zaag P J, Feiner L F, Metselaar R and Devillers M A C 1999 *J. Appl. Phys.* **85** 5100

- [11] Verwey E J W, Haaijman P W, Romeyn F C and Van Oosterhout G M 1950 *Phil. Res. Rep.* **5** 173
- [12] Goyot M 1980 *J. Magn. Magn. Mater.* **18** 925
- [13] Ponpandian N, Balaya P and Narayanasamy A 2002 *J. Phys.: Condens. Matter* **14** 3221
- [14] Li S, Liu L, John V T, O'Connor C J and Harris V G 2001 *IEEE Trans. Magn.* **37** 2350
- [15] Shi Y, Ding J and Yin H 2000 *J. Alloys Compounds* **308** 290
- [16] Cote L J, Teja A S, Wilkinson A P and John Zhang Z 2003 *Fluid Phase Equilib.* **210** 307
- [17] Li S, John V T, O'Connor C, Harris V and Carpenter E 2000 *J. Appl. Phys.* **87** 6223
- [18] Giri A K, Kirkpatrick E M, Moongkhaklang P, Majetich S A and Harris V G 2002 *Appl. Phys. Lett.* **80** 2341
- [19] Mahajan P R, Patankar K K, Kothale M B, Chaudhari S C, Mathe V L and Patil S A 2002 *Pramana* **58** 1115
- [20] Jonker G H 1959 *J. Phys. Chem. Solids* **9** 165
- [21] Na J G, Lee T D and Park S J 1992 *IEEE Trans. Magn.* **28** 2433
- [22] Na J G, Kim M C, Lee T D and Park S J 1993 *IEEE Trans. Magn.* **29** 3520
- [23] Chinnasamy C N, Jeyadevan B, Perales-Perez O, Shinoda K, Tohji K and Kasuya A 2002 *IEEE Trans. Magn.* **38** 2640
- [24] Sivakumar N, Narayanasamy A, Shinoda K, Chinnasamy C N, Jeyadevan B and Greneche J-M 2007 *J. Appl. Phys.* **102** 013916
- [25] Cullity B D 1978 *Elements of x-ray Diffraction* (London: Addison-Wesley)
- [26] Murthy V R K and Sobnandari J 1976 *Phys. Status Solidi a* **36** K133
- [27] Rezlescu N and Rezlescu E 1974 *Phys. Status Solidi a* **23** 575
- [28] Irvine J T S, Huanosta A, Velenzuela R and West A R 1990 *J. Am. Ceram. Soc.* **73** 729
- [29] Koops C G 1951 *Phys. Rev.* **83** 121
- [30] Verma A and Dube D C 2005 *J. Am. Ceram. Soc.* **88** 519
- [31] Verma A, Goel T C, Mendiratta R G and Gupta R G 1999 *J. Magn. Magn. Mater.* **192** 271
- [32] Shitre A R, Kawade V B, Bichile G K and Jadhav K M 2002 *Mater. Lett.* **56** 188
- [33] Ranga Mohan G, Ravinder D, Ramana Reddy A V and Boyanov B S 1999 *Mater. Lett.* **40** 39
- [34] Hiti M A 1968 *J. Magn. Magn. Mater.* **164** 231
- [35] Verma A, Thakur O P, Prakash C, Goel T C and Mendiratta R G 2005 *Mater. Sci. Eng. B* **116** 1
- [36] Dias and Moreira R L 1999 *Mater. Lett.* **39** 69
- [37] Baskaran N, Govindaraj G and Narayanasamy A 1997 *Solid State Ion.* **98** 217
- [38] Macedo P B, Moynihan C T and Bosech R 1972 *Phys. Chem. Glasses* **13** 171
- [39] Williams G and Watts D C 1970 *Trans. Faraday Soc.* **66** 80
- [40] Dyre Jeppe C and Schröder Thomas B 2000 *Rev. Mod. Phys.* **72** 873
- [41] Ata-Allah S S, Fayek M K, Sayed H A and Yehia M 2005 *Mater. Chem. Phys.* **92** 278